OXIDATION OF MANGANESE AND DECOMPOSITION OF MnO_2

Stefan Kelzenberg, Norbert Eisenreich, Sebastian Knapp, Andrzej Koleczko, Heike Schuppler

Fraunhofer Institut für Chemische Technologie ICT

Joseph-von-Fraunhofer-Straße 7, 76327 Pfinztal, Germany

stefan.kelzenberg@ict.fraunhofer.de

phone: +49 721 4640 256

Abstract

1 Introduction

Manganese and even more manganese oxides play an important role in many areas. In pyrotechnics, manganese dioxide is used as an oxidiser and manganese may be used as a fuel. Therefore, a good knowledge of the oxidation reaction of manganese and the reduction of manganese dioxide is of fundamental importance. In literature, some studies can be found investigating the decomposition of manganese oxides [3] - [8]. Less information is found on the oxidation of manganese [1][2]. The aim of our studies on oxidation of metals and decomposition of metal oxides [10][11] is to supply kinetical parameters for the hot-spot model that we use to describe thermal interactions in particulate systems [12][13]. Kinetical parameters can be derived from different kinds of measurement. Here, three different apparatus are used.

2 Experiment

To measure the thermal behaviour of the material under consideration, three different apparatus are used: First is a NETZSCH STA 449C Jupiter micro balance that enables simultaneous DSC and TG measurement. For manganese and manganese dioxide, a temperature range from 25 – 1200 °C is used. Only TG measurements can be performed by a TA Instruments TGA Q5000 using a temperature range from 25 – 1000°C. A different technique is the use of in-situ XRD with temperature control. An XRD Bruker – D8 Advance (AXS) instrument can perform 2θ-scans from 20 – 80°, and temperatures from 50 – 1000 °C

Manganese oxide MnO_2 powder was purchased from Sigma Aldrich with a purity >99.99%. Manganese powder was also purchased from Sigma Aldrich with a purity of 99.9% and a mean particle size of $d_{0.5}$ = 24.214 µm and a specific surface area of 0.125 m^2/g (Determined with Malvern Instruments Ltd. Mastersizer 2000).

TG measurements with manganese dioxide were performed at heating rates of 2, 5, 10, 15, and 20 K/min. Oxidation of manganese was investigated at heating rates of 1, 2, 5, 10, 15, and 20 K/min.

3 Results and Discussion

The following steps have been performed for the evaluation of the measured data to receive kinetical parameters. From XRD measurements, the sequence of appearance of the manganese oxides is determined resulting in a reaction scheme. The reaction scheme is necessary for the choice of fit function in the determination of the kinetical parameters. The next step is the determination of the development of the intensity of some characteristic peaks. The intensities are normalized and selected fit function is fitted to the data. Fit parameters are the activation energy and the frequency factor for each reaction step.

Data from TG measurements are normalized with respect to the initial sample mass and the first derivative is determined numerically. Again to these data the fit function is fitted and the activation energy and the frequency factor are determined.

3.1 Decomposition of Manganese Dioxide

Figure 1 shows the results of an XRD measurement of the decomposition of manganese dioxide (MnO_2, Mn(IV)oxide). The step height was 10 K and each step took 48 min to scan from 30° to 60° (2θ). Besides MnO_2, the occurrence of Mn_2O_3 and Mn_3O_4 could be stated resulting in the following reaction scheme

$$MnO_2 \rightarrow Mn_2O_3 \rightarrow Mn_3O_4$$

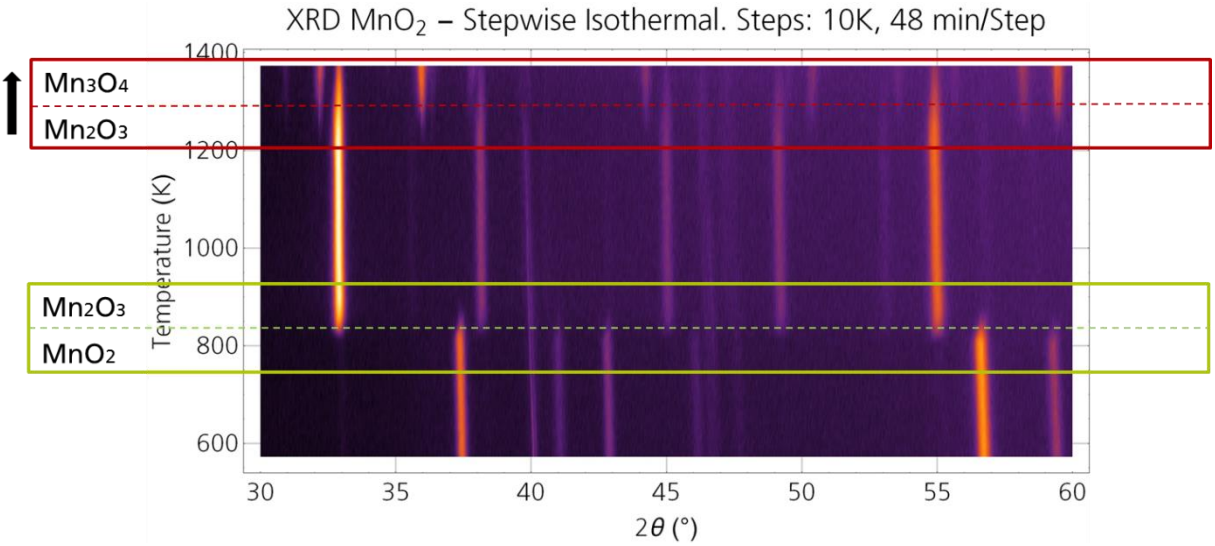

Figure 1: XRD of manganese dioxide steps of 10 K in N_2

In a first step the intensities of some MnO_2 peaks are determined. Figure 2 gives the normalized peak intensities and the corresponding fit for the first step of the reaction scheme $MnO_2 \rightarrow Mn_2O_3$ assuming a first order chemical reaction (see Eq. (1)).

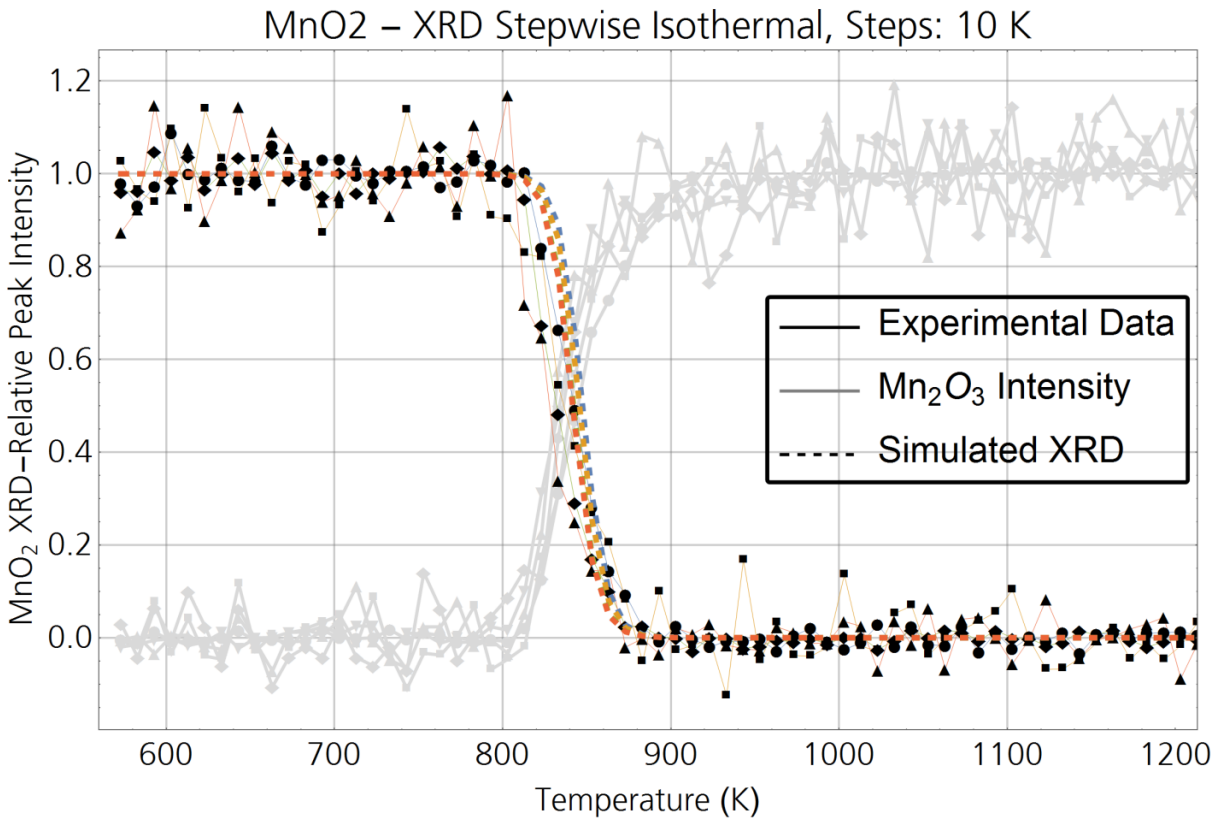

Figure 2: Evaluation of MnO_2 peaks in XRD measurement for the determination of reaction parameters for the first reaction step of the decomposition of MnO_2

The results of the fit are given in Table 1.

Reaction step	Reaction model	Fit parameter	
$6MnO_2 \rightarrow 3Mn_2O_3 + 3O_2$	First order chemical reaction	E_A = 24250 K	Log(Z) = 8.8

Table 1: Kinetical parameters from the evaluation of MnO_2 peaks in XRD measurement

TG measurements were performed in nitrogen with heating rates of 2, 5, 10, 15, and 20 K/min. The normalized data are shown in Figure 3. Two reaction steps are clearly visible.

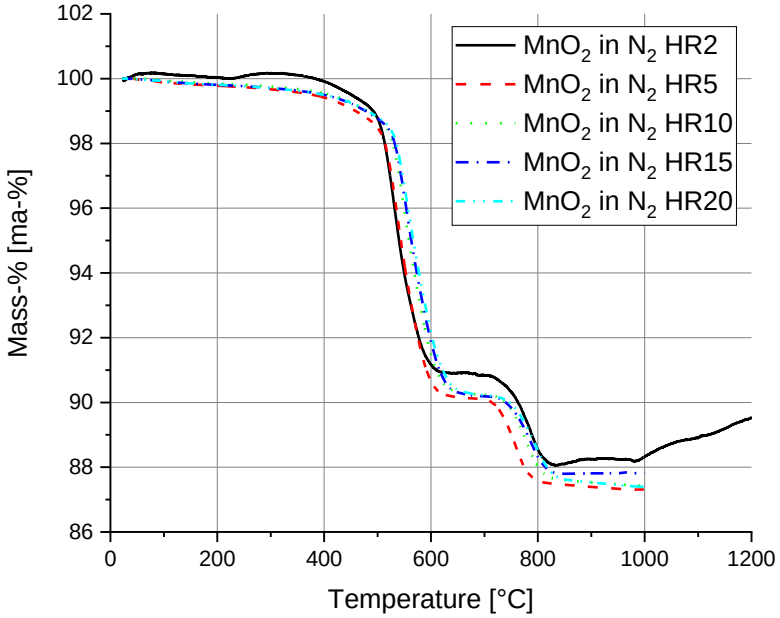

Figure 3: TG of MnO_2 with heating rates of 2, 5, 10, 15, 20 K/min in N_2

From TG data the mass loss for each step can be determined. The values are given in Table 2.

Reaction step	Mass loss* theory	experiment
$6MnO_2 \rightarrow 3Mn_2O_3 + 3O_2$	9.20%	~9%
$3Mn_2O_3 \rightarrow 2Mn_3O_4 + 0.5O_2$	3.07%	~3%

*relative to the mass of manganese dioxide

Table 2: Reaction steps and theoretical mass loss in the decomposition of manganese dioxide (MnO_2)

Figure 4 displays an example for the derivative of TG curve (DTG) at a heating rate of 5 K/min. The peaks of the derivative reflect the steps of TG curve. The peaks are distinct and

the curve of the derivative returns to zero value between the peaks making the fit easier and more stable.

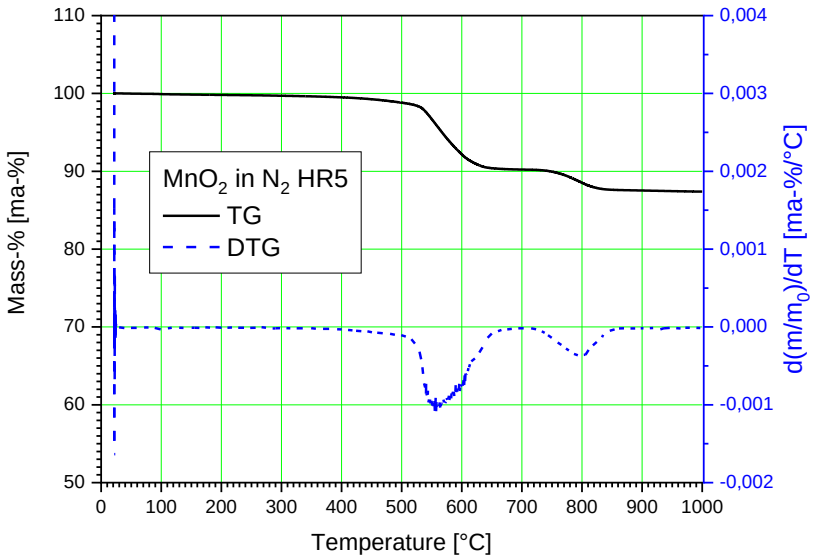

Figure 4: TG and DTG of MnO_2 with a heating rate of 5 K/min in N_2

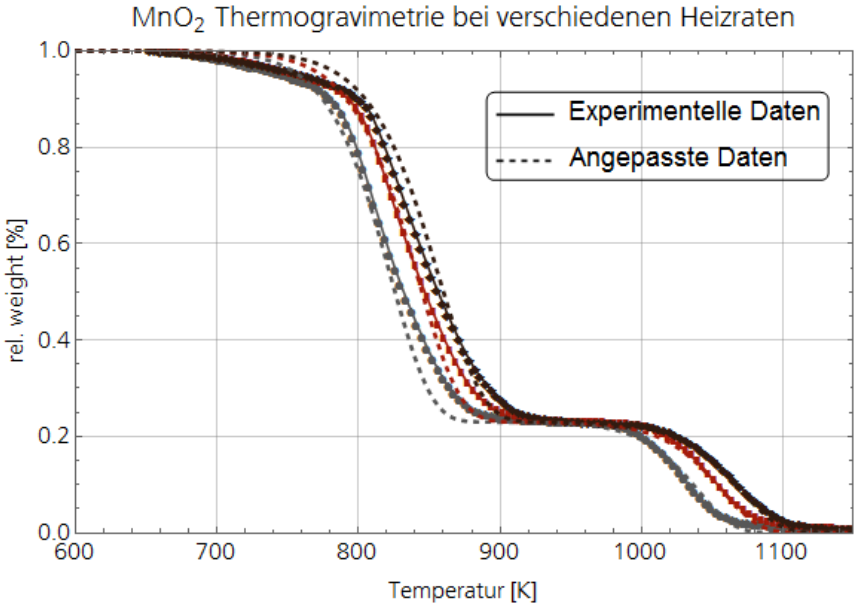

Figure 5: Simultaneous evaluation of TG measurement with different heating rates

Figure 5 shows the results of the fitting procedure using Eq. (1) for both steps and Table 3 gives the values for the activation energy and the frequency factor.

$$\alpha = \frac{1}{1+10^{k}\left(\frac{T_0}{\beta}\left(e^{-\frac{E}{R(T_0+t\beta)}}-e^{-\frac{E}{RT_0}}\right)+te^{-\frac{E}{R(T_0+t\beta)}}+\frac{E}{\beta}\left(Ei\left[-\frac{E}{R(T_0+t\beta)}\right]-Ei\left[-\frac{E}{RT_0}\right]\right)\right)} \quad \text{Eq. (1)}$$

Reaction step	Reaction model	Fit parameter	
$6MnO_2 \rightarrow 3Mn_2O_3 + 3O_2$	First order chemical reaction	E = 23744 K	k = 10
$3Mn_2O_3 \rightarrow 2Mn_3O_4 + 0.5O_2$	First order chemical reaction	E = 42516 K	k = 15.3

Table 3: Kinetical parameters from the evaluation of MnO_2 TG measurement

3.2 Oxidation of Manganese

As the decomposition of MnO_2, the oxidation of manganese runs over several steps. Figure 6 shows the results of XRD measurement giving indication for three reaction steps. The identified substances are Mn, MnO, Mn_3O_4 and Mn_2O_3. The resulting reaction scheme is:

$Mn \rightarrow MnO \rightarrow Mn_3O_4 \rightarrow Mn_2O_3$

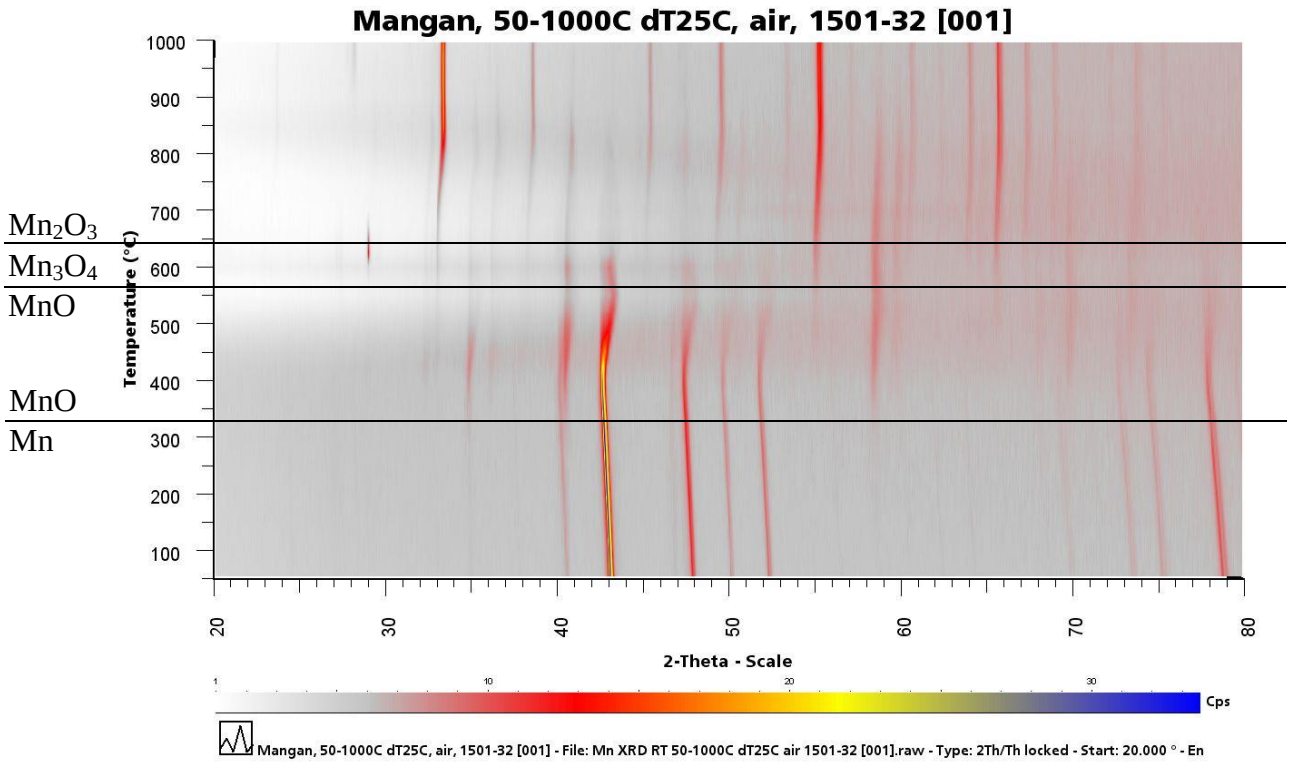

Figure 6: XRD of Manganese steps of 25 K in air.

TG measurements were performed in air with heating rates of 1, 2, 5, 10, 15, and 20 K/min. The normalized data are shown in Figure 7. It seems that the curves show only one step but

the derivatives, an example is given in Figure 8, show several steps and peaks indicating several reaction steps similar to XRD measurements.

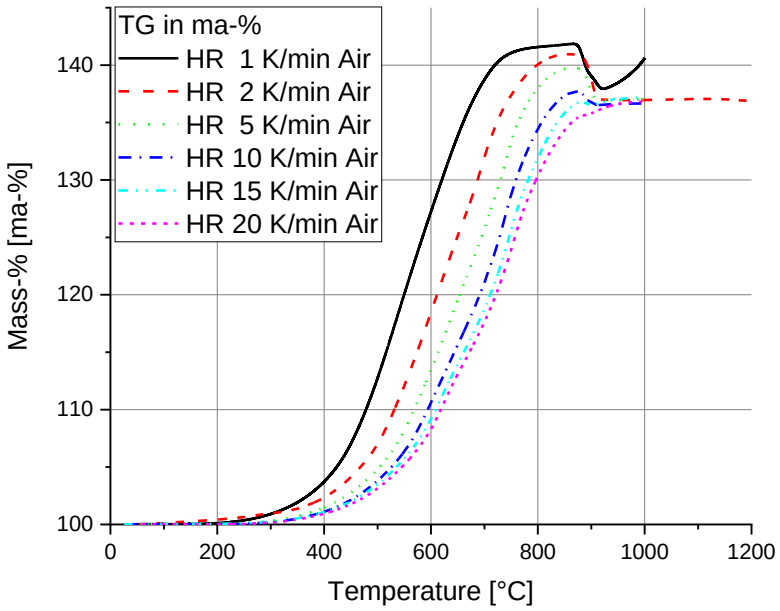

Figure 7: TG of Mn with heating rates of 1, 2, 5, 10, 15, 20 K/min in air

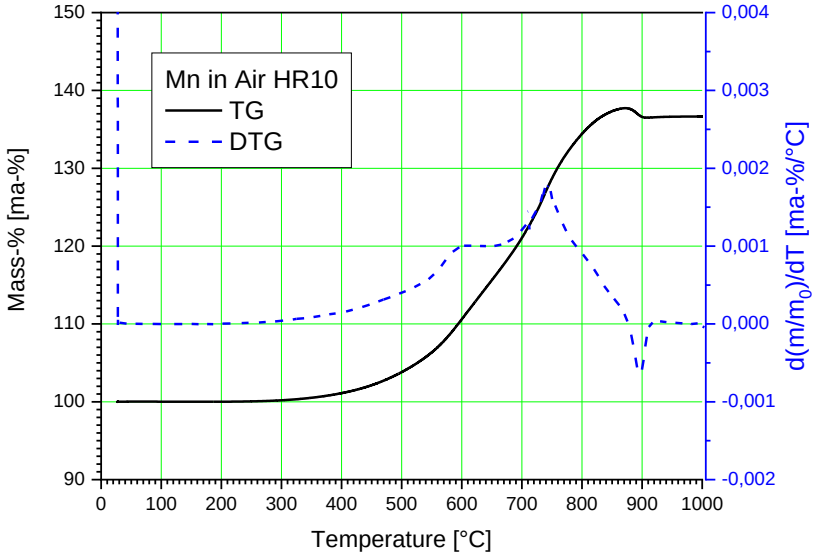

Figure 8: TG and DTG of Mn with a heating rate of 10 K/min in air.

The following reaction scheme can be derived:

$Mn \rightarrow MnO \rightarrow Mn_3O_4 \rightarrow Mn_2O_3 \rightarrow Mn_3O_4$

As reaction steps overlap, the mass loss of the different steps cannot be determined from TG curves directly. Therefore, Table 4 gives only the theoretical values.

Reaction step	Mass change* theory	experiment
$Mn + 0.5O_2 \rightarrow MnO$	29.12%	n.a.
$3MnO + 0.5O_2 \rightarrow Mn_3O_4$	9.71%	n.a.
$2Mn_3O_4 + 0.5O_2 \rightarrow 3Mn_2O_3$	4.85%	n.a.
$3Mn_2O_3 \rightarrow 2Mn_3O_4 + 0.5O_2$	-9.71%	n.a.

*relative to the mass of manganese

Table 4: Reaction steps and theoretical mass change in the oxidation of manganese

It can be assumed that the first reaction step is diffusion-controlled. Therefore, the shrinking core model may be a suitable model for the fitting function. Eq. (2) gives the core radius R_K as a function of temperature. The model is described in detail in [9]. Eq. (3) is the function that has to be fitted to the measured data.

$$R_{K,2}[t] = \frac{1}{2}\left(R_S + \frac{1}{2}\frac{\left(-1-i\sqrt{3}\right)}{\beta R}\exp\left[\frac{-E_D}{RT}\right]\sqrt[3]{x} + \frac{1}{2}\frac{\left(-1+i\sqrt{3}\right)\beta R}{\exp\left[\frac{-E_D}{RT}\right]\sqrt[3]{x}}R_S^2 \right) \qquad \text{Eq. (2)}$$

with

$$x = -\beta^3 R^3 \exp\left[\frac{3E_D}{RT}\right]R_S^3 + 12\beta^2 R^3 a Z_D \exp\left[\frac{2E_D}{RT}\right]R_S T - 12\beta^2 R^2 a Z_D \left[\frac{3E_D}{RT}\right]R_S E_D \Gamma\left[0, \frac{E_D}{RT}\right]$$
$$+2\beta^2 R^2 R_S \exp\left[\frac{2E_D}{RT}\right]\sqrt{6aZ_D\left(-RT + \exp\left[\frac{E_D}{RT}\right]E_D\Gamma\left[0,\frac{E_D}{RT}\right]\right)\left(\beta R \exp\left[\frac{E_D}{RT}\right]R_S^2 - 6aZ_D RT + 6aZ_D \exp\left[\frac{E_D}{RT}\right]E_D\Gamma\left[0,\frac{E_D}{RT}\right]\right)}$$

$$\alpha = \frac{qM_O}{pM_{Me}}\left(1 - \frac{m_{Me}}{m_0}\right) = \frac{qM_O}{pM_{Me}}\left(1 - \left(\frac{R_K}{R_S}\right)^3\right) \qquad \text{Eq. (3)}$$

Because of the complexity of the oxidation reaction and the overlap of several reaction steps, it seems to be more successful to use the first derivative of α. Nevertheless in a first trial only the first reaction step could be fitted. Figure 9 shows the result for the fit of the first derivative

of α to the first derivative of the measured data. Up to about 800 K, the fitted curve is very close to data.

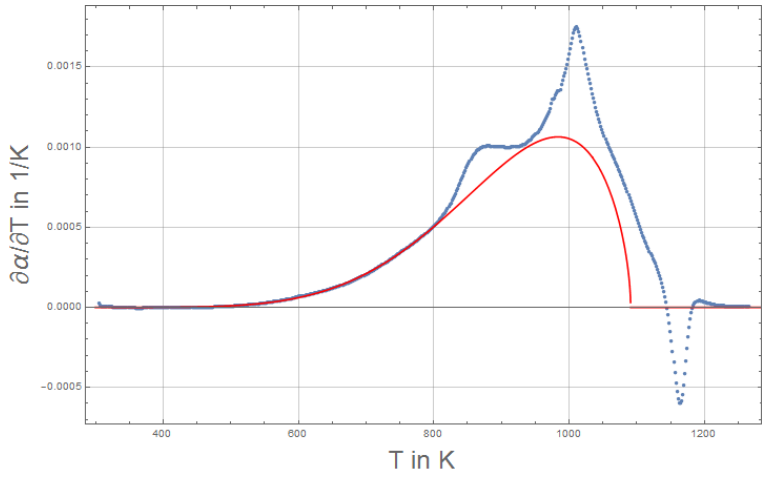

Figure 9: First derivative of mass increase of Mn Oxidation and fitted curve for the first reaction step at a heating rate of 10 K/min

Figure 10 shows the measured data and the values of α calculated with the parameters from the fit of the first derivative.

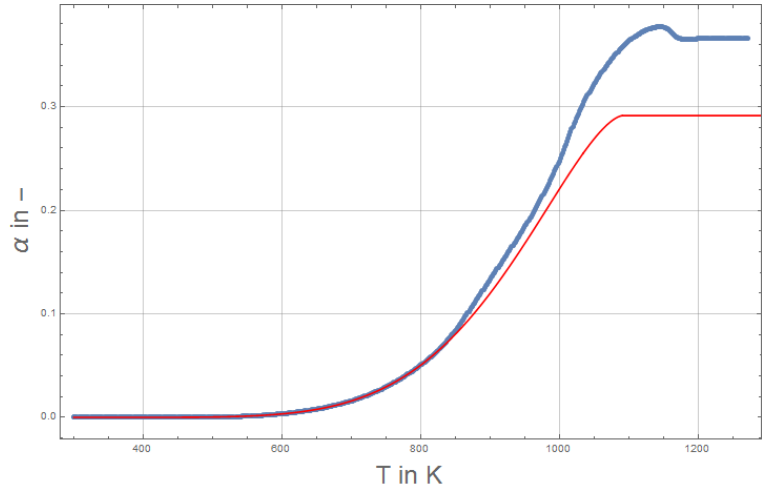

Figure 10: Normalized mass increase of Mn Oxidation and calculated curve for the first reaction step at a heating rate of 10 K/min

As only the first step could be fitted Table 5 gives the parameter values for the first reaction step of manganese oxidation.

Reaction step	Reaction model	Fit parameter	
$Mn + 0.5O_2 \rightarrow MnO$	Shrinking core	$E_D = 98354$	$Log(Z_D) = -3.86$
$3MnO + 0.5O_2 \rightarrow Mn_3O_4$	Shrinking core		
$2Mn_3O_4 + 0.5O_2 \rightarrow 3Mn_2O_3$	Shrinking core		
$3Mn_2O_3 \rightarrow 2Mn_3O_4 + 0.5O_2$	First order chemical reaction		

Table 5: Kinetical parameters from the evaluation of MnO_2 TG measurement

4 Outlook

XRD and TG measurements are performed for the reduction of manganese dioxide and the oxidation of manganese. Different heating rates are used in TG. Data were normalized and first derivative build. For manganese dioxide, reaction steps are clearly separated and could be fitted with first order chemical reaction. In the case of the oxidation of manganese, the situation is much more complicate because of the overlap of the reaction steps. Therefore, more effort is necessary to complete the study of the reduction of manganese oxide and the oxidation of manganese.

5 References

[1] J. D. Hem, Chemical Equilibria and Rates of Manganese Oxidation, in: S. D. Udall, T. B. Nolan, Chemistry of Manganese in Natural Water, Geological Survey Water-Supply Paper 1667-A, US Government Printing Office, Washington, **1963**.

[2] R. Pompe, Some Oxidation Properties of Manganese and its Lower Oxides, Acta Chimica Scandinavica A30, **1976**, 370 – 374.

[3] G. J. W. Kor, The Thermal Decomposition of Mn_2O_3 and the Reduction of Mn_3O_4 by C and CO, Metallurgical Transactions B, 9B, **1978**, 307 – 311.

[4] K. Terayama, M. Ikeda, Study on Thermal Decomposition of MnO_2 and Mn_2O_3 by Thermal Analysis, Transactions of the Japan Institute of Metals, 24 (11), **1983**, 754 – 758.

[5] Chen Qiyuan, Chen Xinmin, DSC Studies on the Kinetics of Decomposition of Manganese Dioxide, Thermochimica Acta, 123, **1988**, 61 – 71.

[6] M. I. Zaki, M. A. Hasan, L. Pasupulety, K. Kumari, Thermochemistry of Manganese Oxides in Reactive Gas Atmospheres: Probing Redox Compositions in the Decomposition Course $MnO_2 \rightarrow MnO$, Thermochimica Acta, 303, **1997**, 171 – 181.

[7] S. M. Pourmortazavi, S. S. Hajimirsadeghi, I. Kohsari, M. Fathollahi, S. G. Hosseini, Thermal Decomposition of Pyrotechnic Mixtures Containing either Aluminum or Magnesium Powder as Fuel, Fuel, 87, **2008**, 244 – 251.

[8] N. Birkner, A. Navrotsky, Thermodynamics of Manganese Oxides: Effects of Particle Size and Hydration on Oxidation-Reduction Equilibria among Hausmannite, Bixbyite, and Pyrolusite, American Mineralogist, 97, **2012**, 1291–1298.

[9] S. Kelzenberg, N. Eisenreich, S. Knapp, V. Weiser, Shrinking Core Model to Describe Metal Particle Oxidation from Thermal Analysis Data, International Journal of Energetic Materials and Chemical Propulsion, 15 (1), **2016**, 35–48.
[10] S. Knapp, N. Eisenreich, V. Kuchenreuther-Hummel, S. Kelzenberg, A. Koleczko, H. Schuppler, Thermogravimetric Analysis of Molybdenum Oxide (MoO_3) Decomposition, 47th International Annual Conference of ICT, June 28 – July 1, **2016**, 113.
[11] S. Knapp, N. Eisenreich, S. Kelzenberg, E. Roth, V. Weiser, Modelling of Thermite Mixtures, , 48th International Annual Conference of ICT, June 27 – 30, **2017**, 24.
[12] G. Langer, N. Eisenreich, Hot Spots in Energetic Materials, Propellants, Explosives, Pyrotechnics, 24, **1999**, 113-118.
[13] S. Knapp, V. Weiser, S. Kelzenberg, N. Eisenreich, Modeling Ignition and Thermal Wave Progression in Binary Granular Pyrotechnic Compositions, Propellants, Explosives, Pyrotechnics, 39, **2014**, 423-433.